British Journal of Pharmacology

British Journal of Pharmacology (2018) **175** 4121–4136 4121

RESEARCH PAPER

In vitro and *in silico* analysis of the effects of D_2 receptor antagonist target binding kinetics on the cellular response to fluctuating dopamine concentrations

Correspondence Elizabeth C. M. de Lange, Department of Pharmacology, Leiden Academic Centre for Drug Research, Leiden, Netherlands. E-mail: ecmdelange@lacdr.leidenuniv.nl

Received 4 July 2017; **Revised** 17 June 2018; **Accepted** 25 June 2018

Wilhelmus E A de Witte[1], Joost W Versfelt[1], Maria Kuzikov[2], Solene Rolland[3], Victoria Georgi[3], Philip Gribbon[2], Sheraz Gul[2], Dymphy Huntjens[4], Piet Hein van der Graaf[1,5], Meindert Danhof[1], Amaury Fernández-Montalván[3,6], Gesa Witt[2] and Elizabeth C M de Lange[1]

[1]Department of Pharmacology, Leiden Academic Centre for Drug Research, Leiden, Netherlands, [2]ScreeningPort, Fraunhofer Institute for Molecular Biology and Applied Ecology, Hamburg, Germany, [3]Global Drug Discovery, Bayer Healthcare Pharmaceuticals, Berlin, Germany, [4]Janssen R&D, Janssen Pharmaceutica NV, Beerse, Belgium, [5]QSP, Certara, Canterbury, UK, and [6]Servier Research Institute, Croissy-sur-Seine, France

BACKGROUND AND PURPOSE

Target binding kinetics influence the time course of the drug effect (pharmacodynamics) both (i) directly, by affecting the time course of target occupancy, driven by the pharmacokinetics of the drug, competition with endogenous ligands and target turnover, and (ii) indirectly, by affecting signal transduction and homeostatic feedback. For dopamine D_2 receptor antagonists, it has been hypothesized that fast receptor binding kinetics cause fewer side effects, because part of the dynamics of the dopaminergic system is preserved by displacement of these antagonists.

EXPERIMENTAL APPROACH

Target binding kinetics of D_2 receptor antagonists and signal transduction after dopamine and D_2 receptor antagonist exposure were measured *in vitro*. These data were integrated by mechanistic modelling, taking into account competitive binding of endogenous dopamine and the antagonist, the turnover of the second messenger cAMP and negative feedback by PDE turnover.

KEY RESULTS

The proposed signal transduction model successfully described the cellular cAMP response for 17 D_2 receptor antagonists with widely different binding kinetics. Simulation of the response to fluctuating dopamine concentrations revealed that a significant effect of the target binding kinetics on the dynamics of the signalling only occurs at endogenous dopamine concentration fluctuations with frequencies below 1 min^{-1}.

CONCLUSIONS AND IMPLICATIONS

Signal transduction and feedback are important determinants of the time course of drug effects. The effect of the D_2 receptor antagonist dissociation rate constant (k_{off}) is limited to the maximal rate of fluctuations in dopamine signalling as determined by the dopamine k_{off} and the cAMP turnover.

Abbreviations

DMR, dynamic mass redistribution; PPHT, 2-(N-Phenethyl-N-propyl)amino-5-hydroxytetralin; RT, room temperature

DOI:10.1111/bph.14456

Introduction

The potential influence of drug-target association and dissociation kinetics on the time course of drug effects (pharmacodynamics) has led to an increasing interest in the use of binding kinetic parameters as a criterion in the selection of drug candidates (Copeland *et al.*, 2006; Zhang and Monsma, 2010; Lu and Tonge, 2011; Dahl and Akerud, 2013; Copeland, 2016; Vauquelin, 2016). Although the influence of binding kinetics on the time course of target occupancy has been studied, its exact role in the complex relation between drug dosing and drug effect is potentially complex and not completely understood (Yin *et al.*, 2013; de Witte *et al.*, 2016).

Under distinct circumstances, target binding kinetics can influence the pharmacodynamics directly by affecting the time course of the target occupancy. To what extent this occurs depends on the rate constant values for target association (k_{on}) and dissociation (k_{off}), relative to the pharmacokinetic rate constants characterizing the rates of tissue distribution and elimination. In this regard, additional factors to be taken into consideration are the rate constants characterizing the turnover of the target and the competition with endogenous target ligands. In addition to these direct effects of target binding on the pharmacodynamics, variation in k_{on} and k_{off} can also indirectly influence the pharmacodynamics *via* signal transduction and homeostatic feedback mechanisms, both at the cellular and at the systems level (Kleinbloesem *et al.*, 1987; Francheteau *et al.*, 1993; Landersdorfer *et al.*, 2012; Yin *et al.*, 2013; de Witte *et al.*, 2016).

One target for which the influence of drug-target binding kinetics on *in vivo* drug effects is thought to be relevant is the dopamine **D_2 receptor**. Almost two decades ago, the influence of drug-target binding kinetics on the safety of dopamine D_2 antagonists has been suggested, based on the correlation between the high values of k_{off} and the lack of typical side effects, such as extrapyramidal symptoms (i.e. atypicality) (Meltzer, 2004). This observation led to the hypothesis that quickly dissociating antagonists induce less side effects by allowing displacement from the receptor by fluctuating **dopamine** concentrations and thus preserving part of the dopamine dynamics, which we will refer to as the 'fast-off hypothesis' in this study (Kapur and Seeman, 2000, 2001; Langlois *et al.*, 2012; Vauquelin *et al.*, 2012). These fluctuations in dopamine concentrations occur at various time scales *in vivo*, ranging from hours to microseconds (Young *et al.*, 1998; Schultz, 2007; Vauquelin *et al.*, 2012).

The dopamine D_2 receptor belongs to the class of inhibitory GPCRs. Thus, receptor activation is known to inhibit production of **cAMP**, and cAMP in turn is known to stimulate active **PDE** production, while active PDE stimulates degradation of cAMP. Moreover, GPCR receptor activation can lead to receptor phosphorylation and desensitization as described quantitatively for the β_2-adrenergic receptor (Violin *et al.*, 2008). The production of cAMP is thus regulated by a negative feedback loop, which is a common feature in signal transduction pathways (Ingalls, 2013). Many compounds binding to D_2 receptors that were initially classified as antagonists, were later reported to function as inverse agonists (Hall and Strange, 1997; Bond and IJzerman, 2006). For convenience, in this text, only the terms agonist and antagonist will be used.

In the present study, *in vitro* and *in silico* methods were combined to elucidate the influence of D_2 receptor antagonist target binding kinetics on the cellular response to fluctuating dopamine concentrations and to investigate the fast-off hypothesis. Firstly, experimental methods were developed to quantify the binding kinetics of D_2 receptor antagonists, to support the comparison of signal transduction kinetics to target binding kinetics. Secondly, to investigate the fast-off hypothesis with respect to the competition between antagonists and dopamine, the cellular response kinetics after subsequent exposure to dopamine and D_2 receptor antagonists with varying binding kinetics at different levels of the signalling pathway were measured. A minimal mechanistic model combining D_2 receptor binding kinetics, D_2 receptor turnover, cAMP and active PDE turnover was established to describe cAMP concentration versus time curves in response to D_2 receptor antagonist exposure. Thirdly, the model was used to identify the role of binding kinetics on drug effect for fluctuating dopamine concentrations. The physiological range of dopamine fluctuation time scales was taken into account by using a frequency response analysis (Ang *et al.*, 2011; Ingalls, 2013), a method that can be used to increase the kinetic insight into pharmacokinetic and pharmacodynamic model behaviour, as recently demonstrated (Schulthess *et al.*, 2017). For a more general insight in the influence of binding kinetics on signal transduction, this analysis was expanded to a range of hypothetical turnover rates of cAMP and active PDE.

Methods

This study consists of three parts:

(I) *In vitro* measurements of target binding and signal transduction kinetics: drug-target binding parameters of 17 dopamine D_2 receptor antagonists were measured at room temperature and at 37°C. The *in vitro* response after dopamine pre-incubation was measured for two different biomarkers: cAMP concentrations over time as second messenger and dynamic mass redistribution (DMR) as a composite signalling marker.

(II) Model-based analysis of the *in vitro* cAMP antagonist response curves: a minimal mechanistic model was developed to describe the cAMP responses of the antagonists, based on the target binding kinetics as determined in part I.

(III) Frequency response analysis: simulations of the predicted *in vivo* response to fluctuating dopamine concentrations. The mechanistic model was used to simulate the cAMP response to dopamine concentrations that fluctuate according to a sine-wave pattern with a range of physiologically relevant frequencies between $2*10^{-6}$ min^{-1} and 7 min^{-1}. The fluctuation amplitude of cAMP, compared to dopamine, was used to summarize the cAMP response.

In vitro measurements of target binding and signal transduction kinetics

Equilibrium and kinetic probe competition assay (ePCA and kPCA). Affinity and kinetic binding parameters for the 17 studied antagonists (see Table 1) were measured with a

Table 1

Kinetic and affinity parameters (k_{on}, k_{off} and K_D) for the D_2 receptor antagonists used to develop the models presented in this study

Compound ID	#	K_D [M]	SD	k_{on} [1/(M*s)]	SD	k_{off} [1/s]	SD
(-)-Nemonapride	1	9.58E-11	3.26E-12	5.66E + 06	2.73E + 05	5.43E-04	4.46E-05
Bromperidol	2	1.89E-09	7.49E-10	2.26E + 06	9.57E + 05	3.91E-03	1.21E-04
Clozapine	3	5.05E-08	1.28E-08	1.20E + 06	1.44E + 06	5.13E-02	5.74E-02
Domperidone	4	3.04E-09	5.08E-10	1.81E + 05	5.26E + 04	5.37E-04	6.75E-05
Dopamine	5	1.27E-06	5.56E-07	1.88E + 04	2.16E + 04	2.82E-02	3.01E-02
JNJ-37822681	6	9.32E-09	2.71E-09	7.33E + 05	NA	9.54E-03	NA
JNJ-39269646	7	4.87E-08	8.35E-09	4.53E + 06	4.51E + 06	1.79E-01	1.64E-01
Haloperidol	8	3.82E-10	4.98E-11	1.21E + 07	5.18E + 06	4.48E-03	1.37E-03
Olanzapine	9	8.58E-09	3.38E-09	>7.30E + 05	NA	>1.00E-02	NA
Paliperidone	10	5.45E-09	2.07E-09	6.81E + 05	1.83E + 05	3.52E-03	4.14E-04
Pimozide	11	2.55E-10	6.74E-11	3.10E + 05	2.45E + 05	7.08E-05	4.17E-05
Quetiapine	12	1.50E-07	6.94E-08	1.03E + 05	2.04E + 04	1.69E-02	6.07E-03
Remoxipride	13	8.31E-08	3.47E-08	3.28E + 05	NA	3.14E-02	NA
Risperidone	14	7.56E-10	7.62E-11	4.43E + 06	8.54E + 05	3.31E-03	3.09E-04
Sertindole	15	4.07E-09	2.23E-09	7.70E + 05	7.00E + 05	2.35E-03	1.13E-03
Spiperone	16	1.79E-10	4.11E-12	5.44E + 06	1.11E + 06	9.70E-04	1.76E-04
S-(+)-Raclopride	17	6.34E-10	1.15E-10	9.57E + 05	1.81E + 05	5.96E-04	4.62E-06
Ziprasidone	18	1.31E-09	8.40E-11	1.29E + 06	2.01E + 05	1.67E-03	1.55E-04

Data is the average of two kPCA measurements ($N = 2$, $n = 2$) at room temperature. NA, not available

homogeneous time-resolved fluorescence energy transfer (TR-FRET) binding competition method as previously described for the histamine H1 and the GnRH receptors (Schiele *et al.*, 2014; Nederpelt *et al.*, 2016). In this study, Tag-lite® dopamine D_2-labelled cells and a poly-3-phenylhydrazone thiophene (PPHT)-based dopamine D_2 receptor red agonist fluorescent ligand (both from Cisbio, Codolet, France) were used as receptor-tracer pair to be competed with unlabelled test compounds [Tocris Bioscience (Abingdon, UK), TRC, Sigma-Aldrich (St. Louis, MO, USA), Biotrend Chemicals AG (Köln, Germany) or provided by Janssen Pharmaceutica (Beerse Belgium)]. Briefly, frozen cells containing the terbium (Tb^{2+}) labelled D_2 receptor, were thawed, spun down and re-suspended in Tag-lite buffer (Cisbio) to the concentration indicated by the manufacturer and dispensed into Greiner black small volume 384-well microtiter plates already containing the fluorescent tracer (10 nM end concentration) and the antagonists. These compounds were diluted and transferred to the test plates following the procedures described previously (Schiele *et al.*, 2014).

Starting concentrations of the D_2 receptor antagonist dilution series were adapted according to their expected affinity, in order to cover a meaningful dose range (see Supporting Information Figure S1). At least two independent ePCA and kPCA experiments with two replicates each ($N = 2$, $n = 2$) as described above were performed at room temperature and 37°C. For steady state assays, plates were kept in standard tissue culture incubators, whereas for kinetic assays, the temperature control function of the PHERAstar FS™ microtiter plate reader was used. For ePCA, tracer and D_2 receptor-labelled cells were dispensed to the ready-to-use compound plates to a final volume of 5 μL, and the mixture was incubated for 1 to 2 h prior to acquisition of the steady state TR-FRET ratiometric signals (665/620 nm) upon excitation at 337 nm. Normalized values were fitted to a logistic four-parameter model using the Genedata Screener™ software, and K_i values calculated using the Cheng–Prusoff relationship (Cheng and Prusoff, 1973). For kPCA, the tracer was dispensed to the ready-to-use compound plates prior to introducing them into the PHERAstar FS microtiter plate reader. Then the D_2 receptor-labelled cells were added to wells to a final volume of 10 μL using the injector system of the instrument, and kinetic TR-FRET readings were made at time zero and every 21 s or 100 s (depending on whether faster or slower compounds were being measured) for the times indicated in Supporting Information Figure S1. Baseline-normalized kinetic traces were analysed with a competitive binding kinetics model (Motulsky and Mahan, 1984) adapted to deal with normalized- instead of blank-subtracted curves using the Genedata Screener software. Prior to D_2 antagonist testing, binding saturation and kinetic association and dissociation curves for the dopamine D_2 receptor red antagonist fluorescent ligand were recorded ($N = 2$, $n = 3$) as previously described (Schiele *et al.*, 2014; Nederpelt *et al.*, 2016). Subsequently, these curves were fitted to the corresponding models using GraphPad Prism™ in order to obtain the affinity and kinetic constants used as input parameters in the Cheng–Prusoff and Motulsky and Mahan models for Supporting Information Figure S1a (Cheng and Prusoff, 1973).

cAMP assay. CHO/hD_2 and wt-CHO cells were grown in DMEM/F12 with glutamine (without phenol red; Gibco, Dublin, Ireland), 1% heat inactivated FCS, 1× penicillin/streptomycin, 400 μg·mL^{-1} G418. Cells were cultured in humidified atmosphere at 37°C and 5% CO_2 in air.

To gain insight in the activity of known antagonists after binding to the D_2 receptor, changes in the cellular cAMP level were analysed. To allow real time kinetic measurement, a cAMP-biosensor variant pGloSensor™-22F (Promega Corporation) was used, which consists of a cAMP binding domain (cAMP binding domain B from human PKA regulatory subunit type II β) fused to mutant luciferase. Binding of cAMP results in a conformational change and an increase in luminescence signal. The use of the biosensor system provides a method for a real time measurement of changes in the cAMP level in a non-lytic assay format. Cells from a CHO cell line (CHO, RRID:CVCL_VL22) stably transfected with the long isoform of the human dopamine D_2 receptor, CHO/hD_2 cells, were kindly provided by Janssen Pharmaceutica.

CHO/hD_2 cells (15 000/50 μL) were transiently transfected with the pGloSensor-22F plasmid (2 ng·μL^{-1} i.a.) using FuGeneHD transfection reagent (3 μL FuGeneHD: 1 μg DNA plasmid, Promega, Madison, USA). By reaching 70–80% confluency, cells were harvested using Trypsin/EDTA and resuspended in DMEM/F-12/HEPES medium supplemented with 1% fetal calf serum (FCS), pen/strep and 1 mg·mL^{-1} G418. Prior to addition of the pGloSensor-22F plasmid to cells, it was incubated for 20 min with the FuGeneHD transfection reagent at room temperature. By the end of incubation time, the cells and transfection solution were combined, mixed and plated in white, solid bottom 384-well assay plates (Greiner CELLSTAR® 384-well plates). After 24 h of incubation, the transfection mixture was replaced by 20 μL per well DMEM/F-12/HEPES medium with 9% Glo-substrate followed by 2 h incubation at room temperature. To achieve a good signal window, CHO/hD_2 cells were treated with 3 μM **forskolin** for 30 min. Forskolin was used as an activator of the **adenylate cyclase** and therefore for a receptor-independent increase of the cellular cAMP level. In order to monitor antagonist activity against the natural receptor ligand, cells were incubated with 15 nM dopamine for 20 min prior to addition of antagonists. D_2-receptor antagonists were tested in a 10-point dose response (top concentration 10 μM, 1:4 dilutions), and each condition was measured in triplicate. Signal kinetics was detected for a total period of 1 h every 2 min. All compounds were dissolved in DMSO (Carl Roth GmbH + Co. K, Karlsruhe, Germany).

Dynamic mass redistribution (DMR) assay. For DMR measurements (Fang *et al.*, 2008), 10 μL per well cell culture media (DMEM/F12 without phenol red, Gibco) were transferred into an EnSpire-LFC 384– fibronectin coated plate (PerkinElmer, Waltham, USA) and incubated for 30 min. A suspension of CHO/hD_2 cells in cell culture media was prepared, and cells were seeded into the label-free cellular (LFC) plate (1.5×10^4 cells per well), resulting in a final volume of 30 μL per well. The LFC plate was incubated overnight in a humidified atmosphere at 37°C and 5% CO_2 in air.

On the next day, label-free assay buffer (HBSS, Sigma Aldrich, St Louis, MO), 20 mM HEPES (Sigma Aldrich), 0.5% (v/v) DMSO, 0.05% v/v Pluronic (AnaSpec, Fremont, CA, USA) was prepared. Dopamine was diluted in a label-free assay buffer (5 uM, final assay concentration) and dispensed into an intermediate plate (polypropylene 384-well microplate; Greiner Bio-One GmbH, Frickenhausen, Germany). Of each antagonist, a dilution series in DMSO was prepared and transferred into an intermediate plate. Label-free assay buffer was added to the intermediate plate to dilute the antagonists further.

The media was removed from the LFC plate by washing the wells four times with label-free assay buffer (25 μL per well). The total assay volume after the washing step was 30 μL per well. The LFC plate was placed in an EnSpire multimode reader equipped with Corning® Epic® label-free technology (PerkinElmer). After 2 h, a baseline was recorded (10 min) followed by the addition of dopamine or vehicle control (10 μL per well) from the intermediate plate. Antagonist dispensing and mixing were automated using a Janus Workstation (PerkinElmer). A 20 min kinetic DMR measurement was recorded on the EnSpire multimode reader. Directly afterwards, the D_2-receptor antagonists were transferred from the intermediate plate to the LFC plate (10 μL per well), and a 90 min kinetic DMR measurement was initiated on the EnSpire multimode reader.

Model-based analysis of the in vitro cAMP antagonist response curves

Modelling procedure. To obtain a detectable cAMP signal, AC was activated first by forskolin. The dynamics of this activation was recorded in a separate experiment. As the cAMP response to forskolin addition was measured separately from the cAMP response to the D_2-receptor antagonists, the D_2 antagonist response measurements were normalized to the average cAMP response before antagonist addition (baseline). A mechanistic model, based on previous models and mechanistic information from literature (Spence *et al.*, 1995; Hall and Strange, 1997; de Ligt *et al.*, 2000; Cherry and Pho, 2002; Bond and IJzerman, 2006; Violin *et al.*, 2008; Keravis and Lugnier, 2012), combining dopamine-receptor binding kinetics, antagonist-receptor binding kinetics and cAMP as well as active PDE turnover to describe the generation of the cAMP response, was used to simultaneously fit the cAMP data of all antagonists. A diversity of models, with differences in mechanistic detail (Table 2), was tested for their utility to describe the cAMP responses. Model fitting was performed in NONMEM v7.3 using ADVAN9. All values of k_{off}, including the k_{off} of dopamine, were fixed to the values that were measured according to the methods described above, while the K_D values were estimated. Models were selected based on the objective function value (OFV), visual inspection of the individual fits of the experiments and physiological plausibility of the models. The OFV is calculated as −2* the natural logarithm of the likelihood, which is an integrated measure of the deviation of all data points from the model predictions. This enables quantitative and statistical model comparisons for which all experiments and all data points together correspond to what would be called the 'group size' in a more classical statistical analysis. As different sources of data and experiments are combined in this analysis, it is not intuitive to express the number of independent experiments underlying this statistical analysis as N = x, but

Table 2

Overview of the objective function values (OFVs) of the final model and the tested alternative models

#	Model	OFV	Model fit
1	Final model	62 404	Successful
2	+ PKA	62 411	Successful
3	– inverse agonism (k_0)	102 215	Terminated
4	– receptor recycling (RR)	81 594	Terminated
5	+ degradation of dopamine	62 404	Successful
6	– active PDE degradation (k_5)	62 307	Successful
7	+ assumption of fast binding kinetics	67 468	Successful

The changes compared to Model 1 are indicated by the mechanistic detail that was added (+) or removed (–) from Model 1.

it should be noted that only the combined number of measured antagonist k_{off} values (17) and the observations of the cellular response of each antagonist at 10 different concentrations (17*10 = 170) make clear that the data for our model has a large enough 'group size' to make reliable statistical comparisons between models. A schematic overview of the final model structure that was fitted to the cAMP response data (Model 1) is given in Figure 1.

Frequency response analysis: simulations of the predicted in vivo response to fluctuating dopamine concentrations

Dopamine concentrations were varied over time according to a sine wave with various frequencies, a mean concentration of 20 nM and an amplitude of 10 nM. The applied antagonist concentration was 14 nM and the antagonist K_D was 6.9 nM. The LFR_{50} was 1.03, and all system-specific parameters were identical to Table 3. The dopamine fluctuations induce fluctuations in the cAMP concentrations, but the amplitude of these fluctuations is dependent on the frequency of the dopamine fluctuations. To get a complete analysis of the cAMP response to fluctuating dopamine concentrations in the presence of an antagonist and to cover all physiologically relevant frequencies (Young *et al.*, 1998; Schultz, 2007; Vauquelin *et al.*, 2012), a wide frequency range was tested between $2*10^{-6}$ min^{-1} and 7 min^{-1}. The simulated frequencies were 0.002, 0.007, 0.02, 0.07, 0.2, 0.7, 2, 7, 20, 70, 200, 700, 2000 and $7000*10^{-3}$ min^{-1}. The simulations were run for 6000 min plus 25* the period of the dopamine fluctuations, to ensure a stable steady state was reached. For frequencies higher than 1 min^{-1}, a step size parameter and absolute tolerance were added to the lsoda solver, to avoid model instability. As the step size parameter, the period of the dopamine fluctuations was divided by 400 and as absolute tolerance, a value of 10^{-6} was used to ensure better model stability at the higher frequencies. The initial values of the differential equations were set to the approximated steady-state values as given in Supporting Information Data S5.

After the cAMP concentration had reached constant fluctuation around the average steady state (i.e. the mean of the minimal and maximal concentration), the amplitudes of both the dopamine and the cAMP concentrations were converted to amplitudes relative to their average steady state values, and their ratio was defined as the 'cAMP gain', according to Equation 1. This gain is a measure for the degree to which dopamine fluctuations results in cAMP fluctuations, and thus, the degree to which a biological signal encaptured in dopamine fluctuations is transduced. All simulations were performed in Rstudio using the deSolve package and the lsoda differential equation solving method (Soetaert *et al.*, 2010; R Core Team, 2013).

$$Gain\ cAMP = \frac{\frac{amplitude\ cAMP}{average\ steady\ state\ cAMP}}{\frac{amplitude\ dopamine}{average\ steady\ state\ dopamine}}. \quad (1)$$

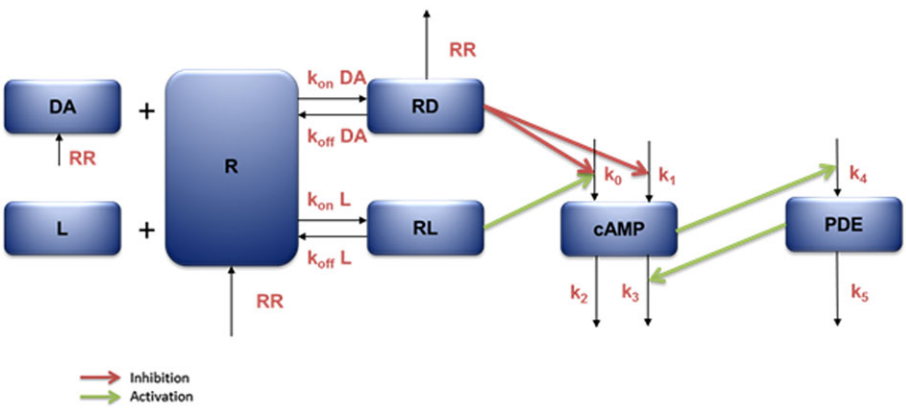

Figure 1

Schematic overview of the structure of the final model (Model 1) used for data fitting and simulations in this study. DA denotes dopamine, L denotes the antagonist, R denotes the D_2-receptor, RD denotes the D_2-receptor-dopamine complex and RL denotes the receptor antagonist complex. RR indicates receptor recycling; the internalization (or degradation) of the dopamine-receptor complex and the resurfacing (or synthesis) of the unbound receptor and dopamine. Black arrows denote mass transfer, green arrows an activating interaction and red arrows an inhibiting interaction. The equations of Model 1 are given in Supporting Information Data S3.

Table 3

Estimates for the system-specific parameters and their uncertainties from fitting Model 1 to the cAMP response data

Parameter	Value (unit)	RSE (%)
K_D dopamine	10.3 (nM)	4.0
k_{off} dopamine	1.69 (min^{-1})	Input parameter
$DAFR_{50}$	2.25	2.4
R_{tot}	1.74 (nM)	1.3
RR	0.238 (min^{-1})	2.2
k_{0max}	20.5 (AU·min^{-1})	0.50
k_1	4.12 (AU·min^{-1})	0.80
k_2 (active PDE-independent)	0.0334 (min^{-1})	11
k_3 (active PDE-dependent)	0.00882 (nM·min^{-1})	0.20
k_4	0.00882 (min^{-1})	Defined as identical to k_3
k_5	0.0005 (min^{-1})	Input parameter
h	1.77	0.40

Naming of the parameters corresponds to Figure 1. $DAFR_{50}$ denotes the ratio of the total receptor concentration divided by the dopamine-bound receptor concentration that inhibits the maximal cAMP synthesis to 50%; R_{tot} denotes the total receptor concentration; k_{0max} denotes the maximal value of k_0; h denotes the hill factor of the non-linear relationship between D_2-receptor occupancy and cAMP synthesis (k_0). The dopamine k_{off} was based on the *in vitro* measurements, and the chosen values for k_4 and k_5 are described in the text. RSE, relative standard error; AU, arbitrary units.

Materials

Janssen Pharmaceutica (Beerse, Belgium) supplied clozapine, dopamine, forskolin, JNJ-37822681, JNJ-39269646, haloperidol, olanzapine, paliperidone and ziprasidone. Sigma-Aldrich supplied domperidone, dopamine, pimozide, quetiapine, S-(+)-raclopride, risperidone and sertindole. MolPort, (Riga, Latvia) supplied remoxipride and spiperone. Toronto Research Chemicals, Inc., (North York, Canada) supplied bromperidol and (-)-nemonapride.

Nomenclature of targets and ligands

Key protein targets and ligands in this article are hyperlinked to corresponding entries in http://www.guidetopharmacology.org, the common portal for data from the IUPHAR/BPS Guide to PHARMACOLOGY (Harding *et al.*, 2018), and are permanently archived in the Concise Guide to PHARMACOLOGY 2017/18 (Alexander *et al.*, 2017a,b).

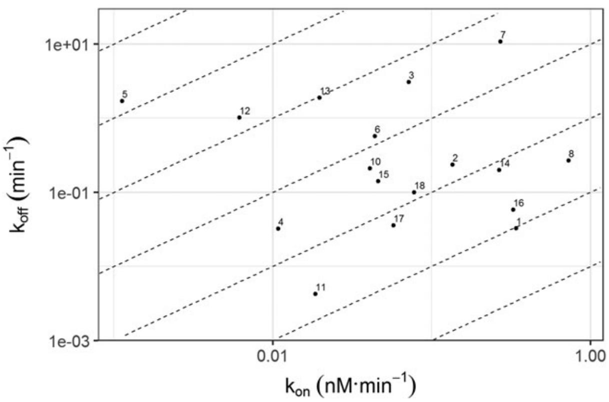

Figure 2

In vitro measurements of k_{on} and k_{off} for each of the measured D_2 antagonists as obtained at room temperature using the kPCA assay. The numbers refer to the compound numbers in Table 1. The diagonal lines indicate constant affinities.

Results

In vitro measurements of target binding and signal transduction kinetics

We have used a novel TR-FRET based assay technology to measure the K_D, k_{on} and k_{off} values of 17 dopamine D_2 receptor antagonists at both room temperature and 37°C. Two datasets were generated using fluorescent derivatives of a fast agonist (PPHT) and a slower antagonist (spiperone). In general, there was a good correlation of the results obtained with both tracers (Supporting Information Figure S1f). Only the PPHT dataset was used to develop the models presented here, since this faster tracer allows the determination of a wider range of rate constants. The results (shown in Figure 2, Table 1, Supporting Information Table S1 and Supporting Information Table S2) are in good agreement with previously published reports that used radioligand binding, as shown in Supporting Information Figure S1f (Leysen and Gommeren, 1986; Freedman *et al.*, 1994; Toll *et al.*, 1998; Seeman and Tallerico, 1998; Kapur and Seeman, 2000; Richelson and Souder, 2000; Kongsamut *et al.*, 2002; Kroeze *et al.*, 2003; Burstein *et al.*, 2005; Langlois *et al.*, 2012; Wood *et al.*, 2015; Klein Herenbrink *et al.*, 2016). Figure 2 shows that the D_2 receptor antagonists evaluated in this study had diverse combinations of k_{on} and k_{off} values and that none of them had a combined low k_{on} and low k_{off} value.

For compounds with higher dissociation rates than the competing fluorescent ligand ($k_{off} \geq 0.01\ s^{-1}$), the precision of the k_{off} estimates is lower, and in some cases, only the lower limit could be identified. However, for the experiments and model fits in this study, the exact value of the k_{off} has less influence on the cAMP concentration for fast compared to slow dissociating compounds and a low precision for high k_{off} values is thus acceptable for the scope of this study. Moreover, it should be noted that for practical reasons, the binding parameters are estimated as mean and SDs. This assumes a normal distribution, which can extend to negative numbers. To prevent this, estimation of geometric mean and geometric SD would have been more appropriate. This assumption only makes a difference where a significant part of the assumed normal distribution is negative, which again is mainly the case for the fast dissociating compounds for which the exact value of the k_{off} is less influential on model performance.

Our cAMP and DMR measurement provide a new and extensive set of signal transduction data for 17 D_2 receptor antagonists. Figure 3 shows the measured cAMP concentrations during the complete time course of a typical experiment with- and a control experiment without dopamine D_2-receptor transfection. For comparison, the DMR responses are given in Supporting Information Data S2. In Figure 4, the complete set of measured cAMP time courses for all 17 D_2 receptor antagonists at 10 different concentrations is given, together with their model fits. The data in Figure 4 show that the antagonists with lower k_{off} values (**pimozide**, **domperidone**, **raclopride**) induce cAMP concentration-time curves for the lower antagonist concentrations with later and lower peak concentrations, compared to faster dissociating compounds (JNJ-39269646, **clozapine**, **olanzapine**). In other words, for the slower dissociating compounds, a more pronounced increase in the time to reach maximal cAMP concentrations with decreasing antagonist concentrations is observed compared to faster dissociating antagonists. However, this trend was not observed in the DMR data (see Supporting Information Data S2).

Model-based analysis of the in vitro cAMP antagonist response curves

Model selection. A series of related model structures, which differed in mechanistic detail, was evaluated for their utility to describe the cAMP responses (Table 2). From these models, Model 1 was selected as the final one for further analyses. This model selection was based on the lowest OFV and on the goodness of fit, as described in Methods section. In Model 1, all antagonists also functioned as inverse agonists by stimulating cAMP production (see Figure 1), and the inverse agonism efficacy was estimated by the model for each antagonist. Model 1 was compared with alternative models to ensure that Model 1 was the optimal model.

Model 2 incorporated more mechanistic detail compared to Model 1 by including the role of **PKA** in linking the cAMP concentrations to active PDE concentrations. The performance of Model 2 was identical to the performance of the simpler Model 1. In addition, the estimated value of PKA turnover was high compared to cAMP and active PDE turnover, which means that the PKA addition to the model did not introduce any further delay in the response kinetics.

Models 3 and 4 were simplified models compared to Model 1 that excluded inverse agonism and receptor recycling respectively. Models 3 and 4 clearly performed worse than Model 1, as indicated by the much higher OFVs.

Model 5 included dopamine elimination/degradation, but this did not improve the model fit.

Model 6 used a fixed value for k_5 which was set to 0. This model performed slightly (although highly significant: $P < 1*10^{-9}$) better than Model 1. The value of k_5 (0.0005 min^{-1}) in the final model (Model 1) was chosen for a combination of physiological and numerical reasons: setting k_5 to zero as in Model 6 would mean that active PDE is only synthesized and not degraded, which would result in a physiologically implausible infinite increase in active PDE concentrations. Moreover, all other parameter values than k_5 differed maximally 5% between Model 6 and Model 1.

Finally, Model 7 demonstrates the contribution of slow binding kinetics to the model fit of the final model, as the exclusion of slow binding kinetics (k_{off} was set to 10 min^{-1} for all antagonists in Model 7) resulted in a large increase of the OFV ($P < 1*10^{-9}$), compared to Model 1.

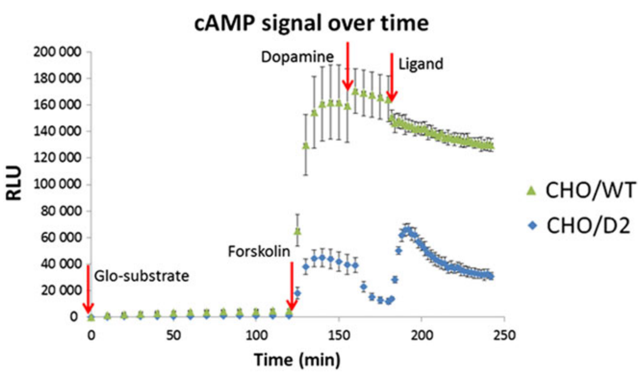

Figure 3

Observed cAMP response during a typical experiment of the Glo-sensor cAMP assay. The red arrows indicate addition of Glo-substrate, forskolin, dopamine and the tested ligand. The green data points were measured in wild type CHO cells, while the blue data points were measured in CHO cells transfected with the dopamine D_2-receptor. N = 1 for CHO/WT, N = 4 for CHO/D_2. RLU, relative light units.

Model fitting. The model fits of Model 1 in Figure 4 demonstrate that the general shape of the cAMP concentration-time curve and the concentration-dependency of the antagonist effect on the cAMP concentration are well captured by the model for all compounds. The equations of Model 1 are given in Supporting Information Data S3. For a few compounds (i.e. clozapine, bromperidol), the peak cAMP concentration or the cAMP concentrations in the terminal phase for the highest antagonist concentrations are underpredicted. The parameter estimates that were the same for all antagonists are given in Table 3, and all parameter estimates are given in Supporting Information Data S3 and Table S3. The uncertainty in the parameter estimates is low, as indicated by the small residual standard errors.

Frequency response analysis: simulations of the predicted in vivo response to fluctuating dopamine concentrations

The simulations of the response to fluctuating dopamine concentrations resulted in a fluctuation pattern of cAMP over

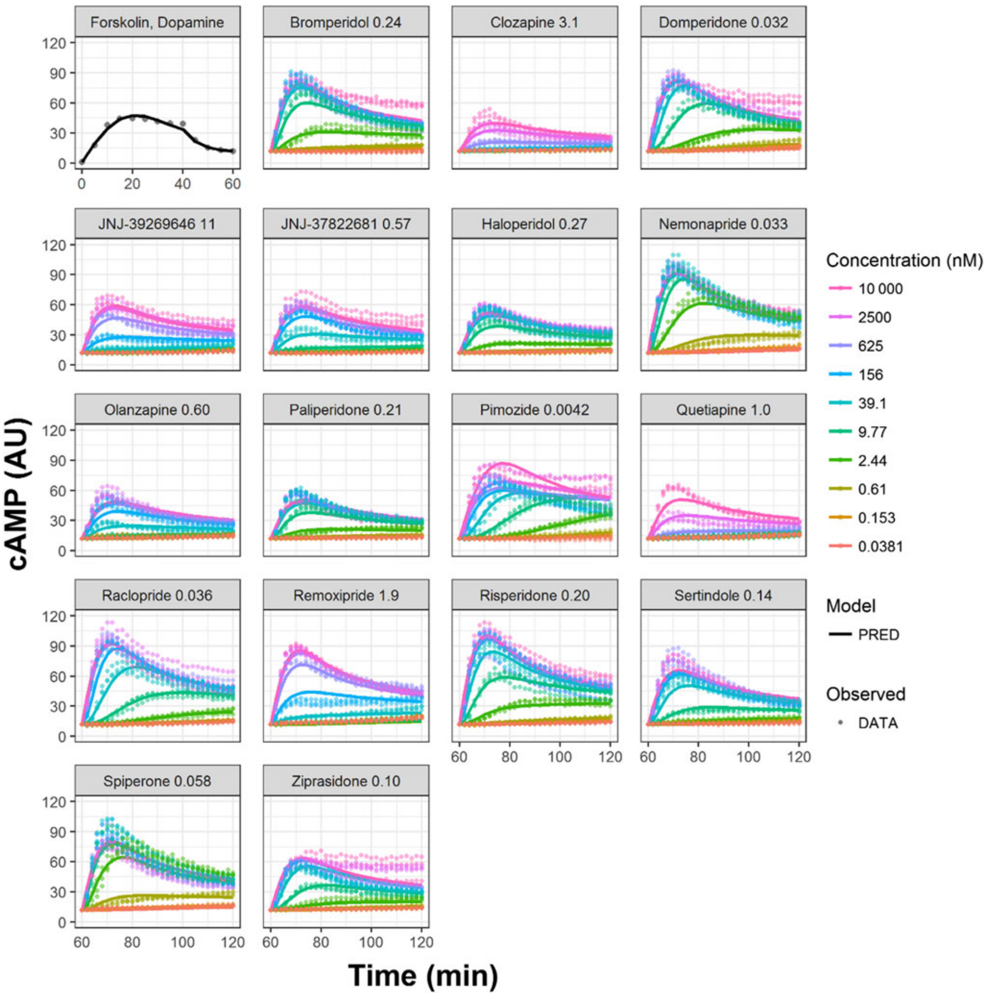

Figure 4

Model fits for all *in vitro* cAMP data as measured in transfected CHO cells. Both the observed (dots) and model-predicted (lines) cAMP signals are included. The colours correspond to the applied concentration in each experiment. The top-left panel shows the cAMP measurements and model predictions for the first 60 min in between forskolin addition and antagonist addition. The lower panels only show the time points after antagonist addition. Each dot represents a single measurement for which n = 1; for each concentration and each time point, three measurements are included. The numbers in the panel labels are the k_{off} values in min^{-1} as used for the model fits for each antagonist.

time for each dopamine fluctuation frequency that was tested. The cAMP fluctuation amplitude was dependent on the frequency, as illustrated in Figure 5.

From these dopamine and cAMP fluctuations, the relative amplitudes and the ratio of these relative amplitudes could be calculated to obtain the cAMP gain (Equation 1, see Methods section) as illustrated in Figure 6. The two simulations in Figures 5 and 6 thus provide two points on the line for an antagonist k_{off} of 2.5 min^{-1} in the graph of Figure 7; at a frequency of 2×10^{-5} min^{-1} and 2 min^{-1}, the cAMP gain is 0.36 and 0.0080 respectively. For a more detailed explanation, see Supporting Information Data S4. The cAMP gain that is obtained by this method is an indication of the extent to which fluctuations in dopamine concentrations lead to fluctuations in cAMP concentrations. By doing so, the cAMP gain informs on the role of dopamine fluctuations on dopamine signalling. A low cAMP gain (cAMP gain $<<$ 1) indicates that only the average dopamine concentrations and not the dopamine fluctuations determine cAMP levels, while a high cAMP gain (cAMP gain $\approx$ 1) indicates that both the average dopamine concentrations and the dopamine fluctuations determine cAMP levels.

From the frequency response analysis as shown in Figure 7, the following was observed:

If dopamine fluctuations occur slowly, the cAMP response has a steady gain (i.e. the cAMP fluctuations have a constant amplitude) for frequencies lower than $1*10^{-5}$ min^{-1} in Figure 7. This gain is increased for intermediate frequencies (between $1*10^{-4}$ and 0.1 min^{-1}) and decreases steeply for higher frequencies. The influence of drug-target binding kinetics on the transduction of dopamine fluctuations into cAMP fluctuations is limited to intermediate frequencies between $1*10^{-4}$ and 0.1 min^{-1} of dopamine fluctuations.

The model-based frequency response analysis allowed characterization of the cAMP response to a wide range of dopamine fluctuation frequencies (as shown in Figure 7). This analysis identified the influence of each model parameter on the cAMP response. The cAMP gain versus dopamine fluctuation frequency graphs as shown in Figure 7 are dependent

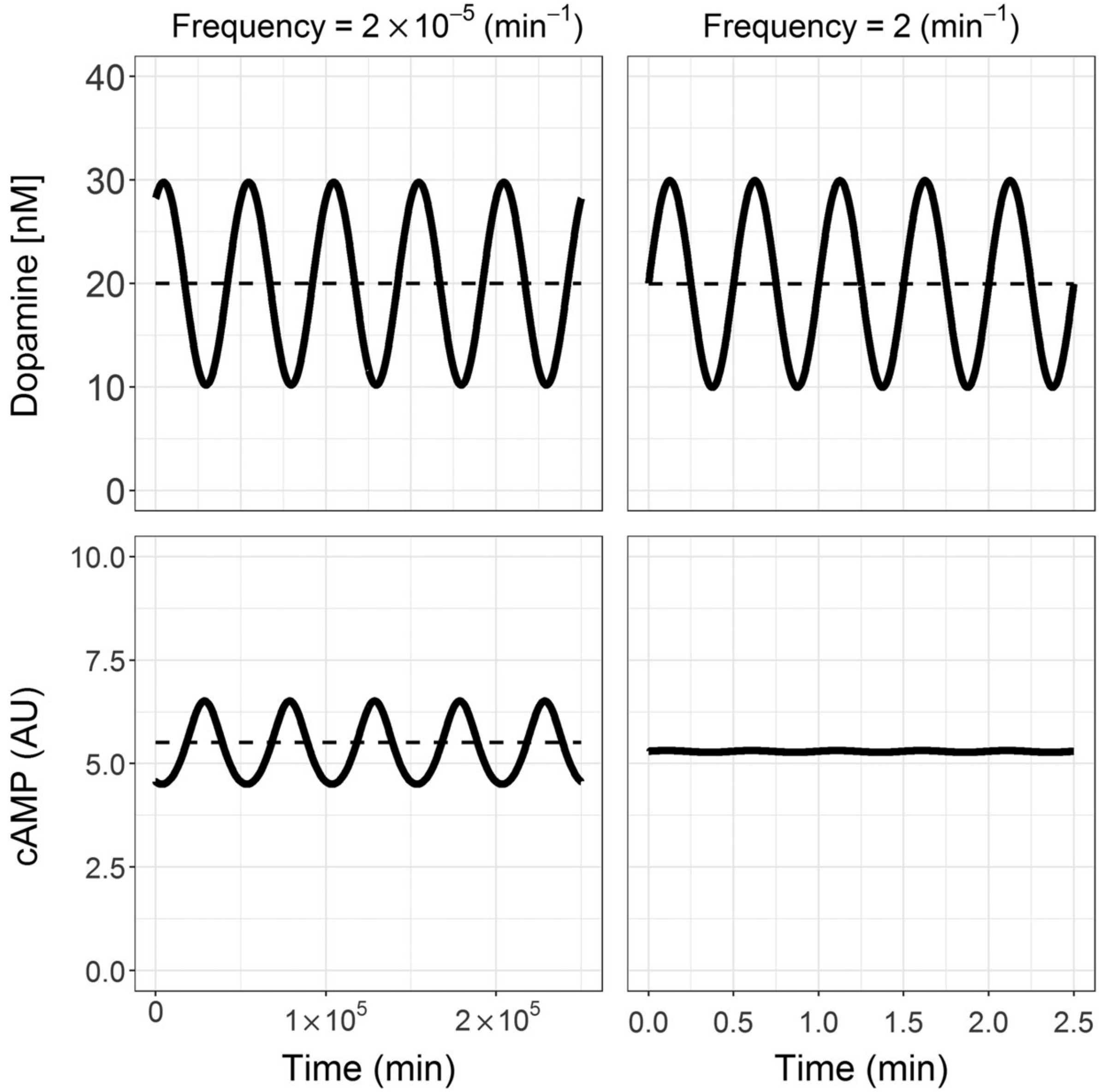

Figure 5

Examples of simulations for low (left-hand plots) and high (right-hand plots) frequency fluctuations of dopamine concentrations. The dashed lines indicate the average steady state values of the fluctuations, which are calculated as the mean of the maximal and the minimal concentrations. Note the different time scales on the left compared to the right plots. The antagonist k_{off} was 2.5 min^{-1} for these simulations.

on the antagonist k_{off} and can have up to three characteristic frequencies around which the gain changes. The positions of the characteristic frequencies are dependent on the parameter values, as discussed below, and have been derived empirically from the gain versus frequency plot as the frequencies at which the cAMP gain starts to change. These frequencies were numbered cf_1, cf_2 and cf_3, as indicated in Figure 7. From the lowest dopamine fluctuation frequencies to cf_1, the cAMP gain is independent of the antagonist k_{off} and does not change with increasing frequency, until cf_1 is reached where the gain increases towards a new plateau value. The frequency at which the cAMP gain declines to a new plateau value, cf_2, is dependent on the antagonist k_{off} and cannot be observed for high-k_{off} antagonists, which is shown for k_{off} values between 0.5 and 2.5 min^{-1} (Figure 7). The third characteristic frequency, cf_3, is independent of the antagonist k_{off} and introduces a decline in the cAMP gain that is linear with the increasing frequency.

The influence of the model parameters on the characteristic frequencies was identified by repeating the FRA for different values of each model parameter, as shown in Supporting Information Data S5. As illustrated by Supporting Information Figure S5, the value of cf_1 depends on the value of the active PDE turnover rate constant k_5. This can be understood by considering that the increase in cAMP gain is caused by a reduced negative feedback if the turnover of active PDE is too slow, relative to the fast fluctuations of cAMP. The second characteristic frequency, cf_2, is influenced by the antagonist

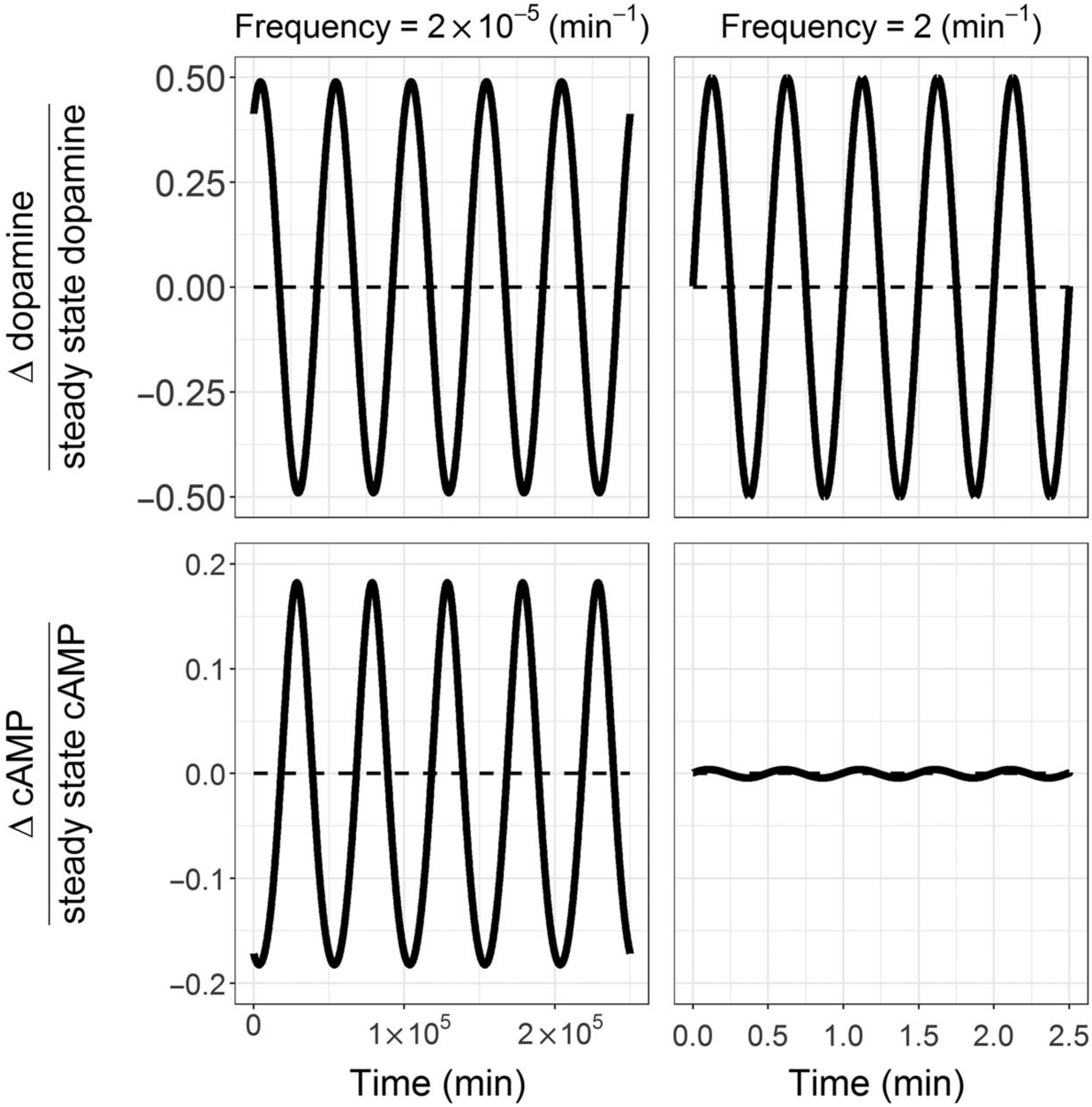

Figure 6

Comparison of relative dopamine and cAMP fluctuations (converted from concentration fluctuations) with average steady state values. The δ sign refers to the difference between the concentration and the average steady state concentration. From these data, the gain can be identified according to Equation 1, which is approximately 0.36 for the left-hand plots and 0.0080 for the right-hand plots. The antagonist k_{off} was 2.5 min^{-1} for these simulations.

k_{off} and by the antagonist concentration, as illustrated in Supporting Information Figure S8. The role of the antagonist k_{off} can be explained by the slow displacement of antagonists with a low k_{off} value and the consequently reduced fluctuation of dopamine receptor occupancy. The role of the antagonist concentration can be explained by the higher antagonist receptor occupancy and the relatively lower influence of fluctuating dopamine concentrations on the antagonist receptor occupancy for higher antagonist concentrations. The third characteristic frequency, cf_3, is determined by both the cAMP turnover and the dopamine k_{off}, as shown in Supporting Information Figures S6 and S7 respectively. These parameters determine the turnover of cAMP and dopamine receptor occupancy, respectively, and the slowest turnover is thus rate limiting for the eventual turnover of cAMP and the maximal frequency of dopamine fluctuations that can be translated into cAMP fluctuations without a declining fluctuation amplitude. In summary, if k_5 (active PDE turnover) increases, cf_1 increases, if the antagonist concentration or k_{off} increases, cf_2 increases and if k_3 (cAMP turnover) increases, cf_3 increases.

Overall, the translation of fluctuating dopamine concentrations into fluctuation of cAMP concentrations is inhibited to a larger extent by antagonists with a low k_{off} value

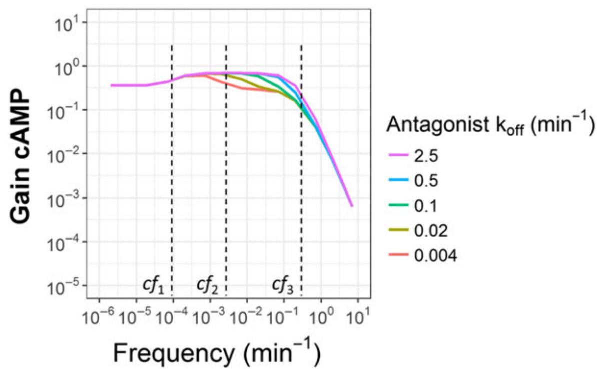

Figure 7

Frequency response analysis of the relative amplitude of cAMP fluctuations normalized to the relative amplitude of dopamine fluctuations (gain). The frequency on the *x*-axes denotes the frequency of the dopamine concentration sine wave that has been used as input for the simulations. The different colours represent different dissociation rate constants (k_{off}) for the antagonist. The applied antagonist concentration was 14 nM while the antagonist K_D was 6.9 nM for all simulations in both plots. The applied dopamine concentrations had a median value of 20 nM and an amplitude of 10 nM. The value of k_{on} changed simultaneously with k_{off} such that the K_D was constant. The dashed lines indicate characteristic frequencies for the red line (k_{off} = 0.004 min^{-1}) at which the gain increases (cf_1) and decreases (cf_2) to new plateau values and decreases linearly with increasing frequencies (cf_3).

compared to antagonists with a high k_{off} value. However, this role of the antagonist k_{off} is only present if the dopamine fluctuation frequency is not too high (i.e. higher than cf_3) to be translated and not too slow (i.e. lower than cf_2) to be able to displace even a slow dissociating antagonist.

Discussion

In this study, we developed a minimal mechanistic model that describes the cellular effects of dopamine D_2 receptor antagonism on cAMP turnover, including dopamine and antagonist receptor binding kinetics as well as active PDE turnover. The model was able to describe successfully *in vitro* binding and cAMP concentration-time profiles data obtained for 17 D_2 receptor antagonists. Compared to fast dissociating antagonists, slowly dissociating D_2 receptor antagonists lead to a reduced response to fluctuating dopamine concentrations as previously suggested in the fast-off hypothesis (see below) for dopamine antagonists. However, this influence of antagonist binding kinetics is only observed to antagonists with a lower k_{off} value than 0.5 min^{-1} and to dopamine fluctuation frequencies higher than the antagonist k_{off} and lower than 0.5 min^{-1}. This range is determined by the cAMP turnover, the dopamine k_{off} and the antagonist k_{off}.

Insight into the influence of target binding kinetics on dopamine D_2 receptor antagonism

According to the fast-off hypothesis for dopamine D_2 receptor antagonists, extrapyramidal side effects can be avoided if dopamine can displace these antagonists from the receptor (Kapur and Seeman, 2001). According to this hypothesis, the k_{off} of an antagonist needs to be high enough to allow that fast fluctuations of dopamine concentration result in the same effects in terms of dopamine D_2-receptor occupancy. However, this hypothesis is only theoretically true under two conditions: (i) fast fluctuations of dopamine receptor occupancy are relevant for the downstream effects of dopamine signalling and (ii) fast fluctuations of dopamine concentrations result in fast fluctuations of dopamine receptor occupancy, if there is no competition for receptor binding. In this study, we demonstrate that both conditions apply for a limited range of dopamine fluctuation frequencies and k_{off} values. Moreover, this study also suggests that the influence of the antagonist k_{off} is of limited extent at therapeutically relevant antagonist occupancies of 60–80%. In fact, fluctuations of endogenous signalling molecules can function as an efficient transduction of the intensity of a constant biological signal, a concept known as frequency encoding. In this case, the average concentration is determining the signal transduction instead of the fluctuations in the signalling molecule concentration. When the fluctuations of dopamine concentrations are not determining the signal transduction, the influence of the antagonist k_{off} on dopamine receptor occupancy fluctuations is unlikely to be relevant for the efficacy or safety of the antagonist. *In vivo*, dopamine concentrations fluctuate with different frequencies. In a dopaminergic synapse, the fastest dopamine fluctuations occur within milliseconds, while slower fluctuations also occur upon activation and deactivation and extra-synaptically (Schultz, 2007). To find out which frequencies of the *in vivo* fluctuations in dopamine concentration can be transduced into cAMP fluctuations, and what is the influence of the antagonist k_{off} thereon, we used simulations to obtain the cAMP gain (i.e. the extent to which dopamine concentration fluctuations are transduced into cAMP concentration fluctuations). To this end, we first obtained a consistent set of parameter values from *in vitro* cAMP response measurements to describe the most important kinetic processes between dopamine fluctuations and cAMP fluctuations.

The k_{off} values that would be necessary for the displacement of dopamine according to the fast-off hypothesis were analysed previously (Vauquelin *et al.*, 2012), but the kinetics of signal transduction were not taken into account in that study. Here, we show that the displacement of D_2 receptor antagonists by dopamine is not generating a fluctuating response if the frequency of fluctuation in D_2 receptor occupancy is higher than what the endogenous signal transduction can translate into a cellular signal, such as cAMP fluctuation. In this study, it is indicated that the rate of endogenous signal transduction is limited both by the dopamine k_{off} and by the cAMP turnover. This can be understood by realizing that each process (antagonist binding, dopamine binding, cAMP turnover) can act as a delay between dopamine concentration fluctuations and cAMP concentration fluctuations, as illustrated in Supporting Information Data S5. This delay attenuates the fluctuations if it is longer than the fluctuation frequency. When this delay is already induced by dopamine binding or cAMP turnover, there is no additional delay imposed by slow antagonist binding, as long as the antagonist binding is faster than dopamine binding and cAMP turnover. Therefore, signal transduction needs to be taken into account to study the influence of binding kinetics on the time course of the drug effect. Our results should not be interpreted as evidence against the relation between D_2 receptor antagonist binding kinetics for their safety profile but as evidence for additional value of signal transduction kinetics, which are not included in the fast-off hypothesis to explain this relationship. It should be noted that alternatives for the fast-off hypothesis are available to explain the difference in extrapyramidal side effects between D_2 receptor antagonists, including the serotonin hypothesis. (Meltzer, 1999)

Extrapolation of in vitro to in vivo antagonism and signal transduction

This study reveals how the relevance of the D_2 receptor antagonist k_{off} depends on the kinetics of signal transduction and negative feedback. In addition, our study provides new insight into the translation of different dopamine fluctuation frequencies into downstream signalling. We speculate that these insights could be used to develop more selective drug treatments towards high or low frequency signalling, for example, for synaptic versus extra-synaptic antagonism. Interestingly, Sykes *et al*. recently demonstrated that a correlation between k_{off} and EPS could not be identified, while a correlation with k_{on} (and probably K_D) could be identified (Sykes *et al*., 2017). On the other hand, a correlation between k_{off} and the effect on prolactin could be identified. While EPS is believed to originate in the neurological synapse, the prolactin response originates in the lactotroph. The differential correlation with k_{off} could therefore also be related with slower dopamine fluctuations in the lactotroph, compared to the synapse. Although we provide a quantitative estimate of the maximal value of k_{off} that could decrease the inhibited transduction of dopamine fluctuations, it should be noted that this value cannot be translated directly into the *in vivo* situation.

Firstly, the temperature at which the signal transduction experiments were performed, room temperature, is not physiological, and most reactions (including drug-target binding kinetics) will be faster at 37°C. However, the difference in binding kinetics between these temperatures is moderate, although highly variable: the ratio of the k_{off} values for the measured D_2 antagonists in this study at 37°C divided by the k_{off} at room temperature was 3.2-fold on average and between 0.10 and 7.4 in the whole dataset, while for k_{on}, this ratio was 2.7 on average and between 0.038 and 6.5 (see Supporting Information Data S1). Therefore, we expect that the kinetics of signal transduction will be different at 37°C compared to our measurements at room temperature. While we do not expect differences of more than one order of magnitude, we cannot exclude larger differences. Although the rate constant of the various kinetic processes might be different *in vivo*, our analysis also identified the role of each rate constant and can thus be used to understand and analyse the *in vivo* situation as well.

Secondly, the analysis of Model 1 in this study only incorporates signal transduction into cAMP and active PDE levels, while in the clinical *in vivo* situation, more transduction steps are involved before the antipsychotic effect of D_2 receptor antagonists is obtained. The differences between the time curves of cAMP and the cellular OD, as measured by DMR (Supporting Information Data S2), provide a first indication of possible differences between the cAMP response and downstream signalling, but the mechanistic interpretation of cellular OD requires more advanced experimental designs (Schröder *et al*., 2010).

Thirdly, the analysis of the cAMP response data with Models 1–7 is not sufficient to obtain a conclusive and comprehensive description of the mechanism(s) underlying the observed cAMP responses. Although various mechanisms were represented by Models 1–7 and fitted to the data, some of these models provide similar fits (e.g. Model 1 and Model 5), and the true mechanism cannot be identified based on these fits alone. To get a better insight into the role of each parameter, we have performed a sensitivity analysis and included the results in Supporting Information Data S5. This shows the identical sensitivity of k_3 and k_4, which explains that these parameters could not be estimated separately. It should be noted that the influence of each parameter as shown in this figure only demonstrates the influence of each parameter if all other parameters have their standard value, which prevents drawing general conclusions of parameter identifiability. Also, the transfected CHO cells used in the *in vitro* measurements of CAMP are not brain cells, and the system-specific parameter values as obtained by the model fit in this study might therefore be different from the *in vivo* situation.

All of these factors might explain why the receptor recycling rate constant as identified here (0.238 min^{-1}) does not correspond to previous more direct estimates of the D_2-receptor degradation rate constant from rat striatum (0.0001 min^{-1}) (Zou *et al*., 1996; Dewar *et al*., 1997). Moreover, our estimate for the dopamine K_D of 10 nM indicates a dominant high-affinity state of the D_2-receptor in the cellular system used for cAMP measurements rather than a dominant low-affinity state which were previously determined as 6.1 and 3650 nM respectively (Durdagi *et al*., 2015). Although this high affinity seems to be close to the *in vivo* affinity (Richfield *et al*., 1989; Flietstra and Levant, 1998), others have found much lower dopamine affinities in CHO cell lines, in agreement with our kPCA results (Sokoloff *et al*., 1990; Freedman *et al*., 1994). This difference might be induced by the experimental conditions during the cAMP experiment, such as the addition of forskolin or the required level of receptor expression, which do not need to be present if the experimental goal is only the measurement of the K_D. Moreover, the K_D values as determined in this study in the kPCA experiments are in the same order of magnitude as those recently published by Sykes *et al*. (2017), although their values are on average around twofold lower than ours, which might be related to the addition of guanine in their experiments. In general, our focus on cAMP signalling and the influence of the experimental conditions prevent from drawing direct conclusions about the influence of D_2-receptor antagonist binding kinetics on *in vivo* extrapyramidal side effects. However, the critical elements in the structure of Model 1 are well supported by previous studies: inverse agonism has been reported for many of the D_2 receptor antagonists as described in Introduction section (Hall and Strange, 1997; Bond and IJzerman, 2006). The active PDE-independent degradation of cAMP has been described before in a more extensive GPCR signalling model (Violin *et al*., 2008) and is also supported by the different molecules that can hydrolyze cAMP (Cherry and Pho, 2002; Keravis and Lugnier, 2012). The two cAMP production rate constants represent the constitutive receptor activity, which is inhibited by inverse agonism (de Ligt *et al*., 2000) and the remaining cAMP production.

Finally, the frequency response analysis that was used here is based on a sine-wave function while the dopamine fluctuations in the brain occur with a more variable frequency and amplitude (Schultz, 2007; Vauquelin *et al*., 2012).

The absolute limit of the influence of binding kinetics on antagonist effects cannot be translated directly into *in vivo* situations, but our findings demonstrate that such a limitation is likely to exist *in vivo* as well and may be expected to be in the order of minutes. Although we focus on extrapyramidal side effects, according to the fast-off hypothesis, these side effects are caused by a dopamine signalling inhibition that is too strong, blocking too much dopamine signalling. Our findings for EPS are thus directly linked to antipsychotic action, if this is mainly mediated by inhibition of dopaminergic signalling. These results indicate that sub-second dopamine fluctuations possibly cannot be translated into cAMP fluctuations and that sub-second k_{off} values might not be required to minimize extrapyramidal side effects. This also questions that antagonists with sub-second dissociation half-lives yield different inhibition of dopamine signalling compared to antagonists with dissociation half-lives in the second-minute range, as suggested before based on theoretical considerations (Vauquelin *et al*., 2012). The relevance of these results are supported by the parameters that were identified to be most influential, the dopamine k_{off} and the cAMP degradation rate constant, which are unlikely to be affected by experimental design.

We have shown that for a common transduction system including an indirect effect and a negative feedback loop, the relevance of fast drug-target dissociation can be limited by the target dissociation of the endogenous ligand and the turnover of the second messenger. The rate constants for dopamine dissociation from the D_2-receptor and cAMP turnover that we have obtained in this study indicate the relevance of signal transduction kinetics for D_2 receptor antagonists. Our study demonstrates that the influence of target binding kinetics on drug effects cannot be fully understood without taking into account signal transduction and feedback kinetics, especially if fluctuating endogenous ligand concentrations are present.

In conclusion, the cellular cAMP response to dopamine D_2 receptor antagonists could be described using a minimal mechanistic model including *in vitro* measured dopamine and antagonist D_2 binding kinetics, in conjunction with synthesis and degradation of cAMP and active PDE. This model revealed that slowly dissociating D_2 receptor antagonists show a reduced transduction of dopamine fluctuations into cAMP fluctuations, compared to fast dissociating antagonists. However, this influence of the dissociation rate constant is limited to dopamine fluctuations that are faster than the k_{off} value of the drug but slower than the dopamine k_{off} value and the cAMP turnover. In general, we conclude that the influence of drug-target binding kinetics on drug effect kinetics is dependent on the dynamics of signal transduction kinetics and that both the turnover of second messengers and the k_{off} value of endogenous ligands might limit the discrimination between fast and slowly dissociating antagonists.

Acknowledgements

This research is part of the K4DD (Kinetics for Drug Discovery) consortium which is supported by the Innovative Medicines Initiative Joint Undertaking (IMI JU) under grant agreement no. 115366. The IMI JU is a project supported by the European Union's Seventh Framework Programme (FP7/2007–2013) and the European Federation of Pharmaceutical Industries and Associations (EFPIA).

Author contributions

The design, performance and evaluation of binding kinetic studies were performed by S.R., V.G. and A.F. The design and performance of cAMP and DMR assays were performed by M.K., G.W., S.G., P.G. and D.H. The design and performance of modelling and simulation were performed by W.d.W., J.V., M.D., P.v.d.G. and L.d.L. All authors wrote and revised the manuscript.

Conflict of interest

The authors declare no conflicts of interest.

Declaration of transparency and scientific rigour

This Declaration acknowledges that this paper adheres to the principles for transparent reporting and scientific rigour of preclinical research recommended by funding agencies, publishers and other organisations engaged with supporting research.

References

Alexander SPH, Christopoulos A, Davenport AP, Kelly E, Marrion NV, Peters JA *et al*. (2017a). The Concise Guide to PHARMACOLOGY 2017/18: G protein-coupled receptors. Br J Pharmacol 174: S17–S129.

Alexander SPH, Fabbro D, Kelly E, Marrion NV, Peters JA, Faccenda E *et al*. (2017b). The Concise Guide to PHARMACOLOGY 2017/18: Enzymes. Br J Pharmacol 174: S272–S359.

Ang J, Ingalls B, McMillen D (2011). Probing the inputoutput behavior of biochemical and genetic systems: system identification methods from control theory (Elsevier Inc.). Methods Enzymol 487: 279–317.

Bond RA, IJzerman AP (2006). Recent developments in constitutive receptor activity and inverse agonism, and their potential for GPCR drug discovery. Trends Pharmacol Sci 27: 92–96.

Burstein ES, Ma J, Wong S, Gao Y, Pham E, Knapp AE *et al*. (2005). Intrinsic efficacy of antipsychotics at human D_2, D_3, and D_4 dopamine receptors: identification of the clozapine metabolite N-desmethylclozapine as a D_2/D_3 partial agonist. J Pharmacol Exp Ther 315: 1278–1287.

Cheng Y-C, Prusoff WH (1973). Relationship between the inhibition constant (KI) and the concentration of inhibitor which causes 50 per cent inhibition (I50) of an enzymatic reaction. Biochem Pharmacol 22: 3099–3108.

Cherry JA, Pho V (2002). Characterization of cAMP degradation by phosphodiesterases in the accessory olfactory system. Chem Senses 27: 643–652.

Copeland RA (2016). The drug-target residence time model: a 10-year retrospective. Nat Rev Drug Discov 15: 87–95.

Copeland RA, Pompliano DL, Meek TD (2006). Drug-target residence time and its implications for lead optimization. Nat Rev Drug Discov 5: 730–739.

Dahl G, Akerud T (2013). Pharmacokinetics and the drug-target residence time concept. Drug Discov Today 18: 697–707.

de Ligt RAF, Kourounakis AP, IJzerman AP (2000). Inverse agonism at G protein-coupled receptors: (patho) physiological relevance and implications for drug discovery. Br J Pharmacol 130: 1–12.

de Witte WEA, Wong YC, Nederpelt I, Heitman LH, Danhof M, van der Graaf PH *et al*. (2016). Mechanistic models enable the rational use of in vitro drug-target binding kinetics for better drug effects in patients. Expert Opin Drug Discov 11: 45–63.

Dewar KM, Paquet M, Reader TA (1997). Alterations in the turnover rate of dopamine D_1 but not D_2 receptors in the adult rat neostriatum after a neonatal dopamine denervation. Neurochem Int 30: 613–621.

Durdagi S, Salmas RE, Stein M, Yurtsever M, Seeman P (2015). Binding interactions of dopamine and apomorphine in D_2High and D_2Low states of human dopamine D_2 receptor (D2R) using computational and experimental techniques. ACS Chem Nerosci 2016; 7: 185–95.

Fang Y, Frutos AG, Verklereen R (2008). Label-free cell-based assays for GPCR screening. Comb Chem High Throughput Screen 11: 357–369.

Flietstra RJ, Levant B (1998). Comparison of D_2 and D_3 dopamine receptor affinity of dopaminergic compounds in rat brain. Life Sci 62: 1825–1831.

Francheteau P, Steimer JL, Merdjan H, Guerret M, Dubray C (1993). A mathematical model for dynamics of cardiovascular drug action: application to intravenous dihydropyridines in healthy volunteers. J Pharmacokinet Biopharm 21: 489–514.

Freedman SB, Patel S, Marwood R, Emms F, Seabrook GR, Knowles MR *et al*. (1994). Expression and pharmacological characterization of the human D_3 dopamine receptor. J Pharmacol Exp Ther 268: 417–426.

Hall DA, Strange PG (1997). Evidence that antipsychotic drugs are inverse agonists at D_2 dopamine receptors. Br J Pharmacol 121: 731–736.

Harding SD, Sharman JL, Faccenda E, Southan C, Pawson AJ, Ireland S *et al*. (2018). The IUPHAR/BPS Guide to PHARMACOLOGY in 2018: updates and expansion to encompass the new guide to immunopharmacology. Nucl Acids Res 46: D1091–D1106.

Ingalls BP (2013). Mathematical Modeling in Systems Biology: an introduction. MIT Press: Cambridge.

Kapur S, Seeman P (2000). Antipsychotic agents differ in how fast they come off the dopamine D_2 receptors. Implications for atypical antipsychotic action. J Psychiatry Neurosci 25: 161–166.

Kapur S, Seeman P (2001). Does fast dissociation from the dopamine D_2 receptor explain the action of atypical antipsychotics? A new hypothesis. Am J Psychiatry 158: 360–369.

Keravis T, Lugnier C (2012). Cyclic nucleotide phosphodiesterase (PDE) isozymes as targets of the intracellular signalling network: benefits of PDE inhibitors in various diseases and perspectives for future therapeutic developments. Br J Pharmacol 165: 1288–1305.

Klein Herenbrink C, Sykes DA, Donthamsetti P, Canals M, Coudrat T, Shonberg J *et al*. (2016). The role of kinetic context in apparent biased agonism at GPCRs. Nat Commun 7: 10842.

Kleinbloesem CH, van Brummelen P, Danhof M, Faber H, Urquhart J, Breimer DD (1987). Rate of increase in the plasma concentration of nifedipine as a major determinant of its hemodynamic effects in humans. Clin Pharmacol Ther 41: 26–30.

Kongsamut S, Kang J, Chen XL, Roehr J, Rampe D (2002). A comparison of the receptor binding and HERG channel affinities for a series of antipsychotic drugs. Eur J Pharmacol 450: 37–41.

Kroeze WK, Hufeisen SJ, Popadak BA, Renock SM, Steinberg S, Ernsberger P *et al*. (2003). H1-histamine receptor affinity predicts short-term weight gain for typical and atypical antipsychotic drugs. Neuropsychopharmacology 28: 519–526.

Landersdorfer CB, He Y-L, Jusko WJ (2012). Mechanism-based population modelling of the effects of vildagliptin on GLP-1, glucose and insulin in patients with type 2 diabetes. Br J Clin Pharmacol 73: 373–390.

Langlois X, Megens A, Lavreysen H, Atack J, Cik M, te Riele P *et al*. (2012). Pharmacology of JNJ-37822681, a specific and fast-dissociating D_2 antagonist for the treatment of schizophrenia. J Pharmacol Exp Ther 342: 91–105.

Leysen JE, Gommeren W (1986). Drug-receptor dissociation time, new tool for drug research: receptor binding affinity and drug-receptor dissociation profiles of serotonin-s2, dopamine-d2, histamine-hi antagonists, and opiates. Drug Dev Res 131: 119–131.

Lu H, Tonge PJ (2011). Drug-target residence time: critical information for lead optimization. Curr Opin Chem Biol 14: 467–474.

Meltzer H (1999). The role of serotonin in antipsychotic drug action. Neuropsychopharmacology 21: 106S–115S.

Meltzer HY (2004). What's atypical about atypical antipsychotic drugs? Curr Opin Pharmacol 4: 53–57.

Motulsky HJ, Mahan LC (1984). The kinetics of competitive radioligand binding predicted mass action by the law of mass action. Mol Pharmacol 25: 1–9.

Nederpelt I, Georgi V, Schiele F, Nowak-Reppel K, Fernández-Montalván AE, Ijzerman AP *et al*. (2016). Characterization of 12 GnRH peptide agonists – a kinetic perspective. Br J Pharmacol 173: 128–141.

R Core Team (2013). R: a language and environment for statistical computing. R Found. Stat. Comput. Vienna, Austria. Available at: http://www.r-project.org/

Richelson E, Souder T (2000). Binding of antipsychotic drugs to human brain receptors focus on newer generation compounds. Life Sci 68: 29–39.

Richfield EK, Penney JB, Young AB (1989). Anatomical and affinity state comparisons between dopamine D_1 and D_2 receptors in the rat central nervous system. Neuroscience 30: 767–777.

Schiele F, Ayaz P, Fernández-Montalván A (2014). A universal, homogenous assay for high throughput determination of binding kinetics. Anal Biochem 468: 42–49.

Schröder R, Janssen N, Schmidt J, Kebig A, Merten N, Hennen S *et al*. (2010). Deconvolution of complex G protein–coupled receptor signaling in live cells using dynamic mass redistribution measurements. Nat Biotechnol 28: 943–949.

Schulthess P, Post TM, Yates J, van der Graaf PH (2017). Frequency-domain response analysis for quantitative systems pharmacology models. CPT Pharmacometrics Syst Pharmacol : 1–13.

Schultz W (2007). Multiple dopamine functions at different time courses. Annu Rev Neurosci 30: 259–288.

Seeman P, Tallerico T (1998). Antipsychotic drugs which elicit little or no parkinsonism bind more loosely than dopamine to brain D_2 receptors, yet occupy high levels of these receptors. Mol Psychiatry 3: 123–134.

Soetaert K, Petzoldt T, Setzer RW (2010). Solving differential equations in R: Package deSolve. J Stat Softw 33: 1–25.

Sokoloff P, Giros B, Martres M-P, Bouthenet M-L, Schwartz J-C (1990). Molecular cloning and characterization of a novel dopamine receptor (D_3) as a target for neuroleptics. Nature 347: 146–151.

Spence S, Rena G, Sweeney G, Houslay MD (1995). Induction of Ca2+/calmodulin-stimulated cAMP phosphodiesterase (PDE1) activity in Chinese hamster ovary cells (CHO) by phorbol 12-myristate 13-acetate and by the selective overexpression of protein kinase C isoforms. Biochem J 310 (Pt. 3): 975–982.

Sykes DA, Moore H, Stott L, Holliday N, Javitch JA, Robert Lane J *et al*. (2017). Extrapyramidal side effects of antipsychotics are linked to their association kinetics at dopamine D_2 receptors. Nat Commun 8: 1–11.

Toll L, Berzetei-Gurske IP, Polgar WE, Brandt SR, Adapa ID, Rodriguez L *et al*. (1998). Standard binding and functional assays related to medications development division testing for potential cocaine and opiate narcotic treatment medications. NIDA Res Monogr 178: 440–466.

Vauquelin G (2016). Impact of target binding kinetics on in vivo drug efficacy: k_{off}, k_{on} and rebinding. Br J Pharmacol 173: 2319–2334.

Vauquelin G, Bostoen S, Vanderheyden P, Seeman P (2012). Clozapine, atypical antipsychotics, and the benefits of fast-off D_2 dopamine receptor antagonism. Naunyn Schmiedebergs Arch Pharmacol 385: 337–372.

Violin JD, DiPilato LM, Yildirim N, Elston TC, Zhang J, Lefkowitz RJ (2008). β2-Adrenergic receptor signaling and desensitization elucidated by quantitative modeling of real time cAMP dynamics. J Biol Chem 283: 2949–2961.

Wood M, Dubois V, Scheller D, Gillard M (2015). Rotigotine is a potent agonist at dopamine D_1 receptors as well as at dopamine D_2 and D_3 receptors. Br J Pharmacol 172: 1124–1135.

Yin N, Pei J, Lai L (2013). A comprehensive analysis of the influence of drug binding kinetics on drug action at molecular and systems levels. Mol Biosyst 9: 1381–1389.

Young AMJ, Ahier RG, Upton RL, Joseph MH, Gray JA (1998). Increased extracellular dopamine in the nucleus accumbens of the rat during associative learning of neutral stimuli. Neuroscience 83: 1175–1183.

Zhang R, Monsma F (2010). Binding kinetics and mechanism of action: toward the discovery and development of better and best in class drugs. Expert Opin Drug Discov 5: 1023–1029.

Zou L-L, Cai S-T, Jin G-Z (1996). Chronic treatment with (-)-stepholidine alters density and turnover of D_1 and D_2 receptors in striatum. Acta Pharmacol Sin 17: 485–489.

Supporting Information

Additional supporting information may be found online in the Supporting Information section at the end of the article.

https://doi.org/10.1111/bph.14456

Data S1 Measurements of binding kinetics and equilibrium binding for antagonists at room temperature and at 37°C.
Table S1 Affinity and kinetic parameters derived from binding equilibrium (ePCA) and binding kinetics (kPCA) measurements. Values represent the mean of two independent experiments with two replicates each (N = 2, n = 2) at 37°C. NA: only one independent experiment could be evaluated. ND: steady state affinities were beyond the concentration range tested or kinetic traces did not fit to the models used for evaluation.
Table S2 Affinity and kinetic parameters derived from binding equilibrium (ePCA) and binding kinetics (kPCA) measurements. Values represent the mean of two independent experiments with two replicates each (N = 2, n = 2) at room temperature. NA: only one independent experiment could be evaluated. ND: binding data did not fit to the models used for evaluation.
Figure S1 Determination of affinity and kinetic parameters for the binding of Dopamine D_2-receptor drugs using the TagLite® homogeneous time resolved fluorescence (HTRF) technology and the equilibrium and kinetic Probe Competition Assays (ePCA and kPCA). Symbols represent the measured data and lines the fits to the corresponding binding models. The compounds indicated with fastD2 and fastD2bu refer to JNJ-37822681 and JNJ-39269646, respectively. (A) Characterization of the PPHT tracer used in ePCA and kPCA at room temperature and at 37°C. The upper panel shows representative steady state titration curves, and the lower panel kinetic association- and dissociation curves at increasing tracer concentrations. HTRF signals were fit to the models specified in the methods section and the resulting binding parameters are indicated in the graphs. The data shown correspond to a single experiment with three replicates. Tracer input parameters used to compute the binding constants of test compounds were averaged from two independent experiments with three replicates each. (B-C) Representative kPCA traces (corresponding to a single experiment with two replicates) of the compounds listed in Table S1 at room temperature (b) and 37°C (c). Compound names are indicated on top of the graphs, Dosing is indicated by the color code specified on the right-hand side. (D-E) ePCA dose-response curves of the compounds listed in Table S1 at room temperature (d) and 37°C (e). Compound names are indicated on top of the graphs The different symbols represent different dilution series. Data shown represent the average of two independent experiment with two replicates each. (F) Comparison of the binding parameters obtained with PPHT-based tracer (agonist) and Spiperone-based tracer (antagonist). (G) Comparison of the binding parameters shown in Tables S1 and S2 with literature data. Reference numbers correspond to the following literature sources: 1 = (Kapur and Seeman, 2000), 2 = (Kroeze *et al*., 2003), 3 = (Burstein *et al*., 2005), 4 = (Langlois *et al*., 2012), 5 = (Kongsamut *et al*., 2002), 6 = (Toll *et al*., 1998), 7 = (Freedman *et al*., 1994), 8 = (Richelson and Souder, 2000), 9 = (Seeman and Tallerico, 1998), 11 = (Leysen and Gommeren, 1986).

Data S2 DMR experimental overview and results for all D_2 antagonists.

Figure S2 Example of the complete DMR versus time curve for 10 μM haloperidol. The time points of addition of dopamine and the ligand (haloperidol in this case) are indicated with the red arrows.

Figure S3 Normalized Dynamic Mass Redistribution (DMR) responses as change in DMR response in picometer compared to the dopamine response after addition of various concentrations of the indicated antagonists. Normalization was performed by subtracting the response per well/replicate at the latest time point after dopamine addition and before antagonist addition (t = 31 min) from the raw DMR traces. Normalization for the dopamine + buffer was performed for each time point by subtracting the mean dopamine + buffer in each experiment/well plate from the normalized DMR traces.

Data S3 Model 1 equations and parameter estimates for all dopamine D_2 antagonists.

Table S3 Parameter estimates from fitting the final model to the cAMP response data. Asterisks indicate parameter values that were not estimated but used as input parameter values. $DAFR_{50}$ denotes the ratio of the total receptor concentration divided by the dopamine-bound bound receptor concentration that inhibits the cAMP synthesis to 50%, LFR_{50} denotes the ratio of the total receptor concentration divided by the antagonist bound receptor concentration that generates the halfmaximal antagonist-dependent cAMP synthesis (i.e. k_0 equals 0.5 * k_{0max}), R_{tot} denotes the total receptor concentration, k0max denotes the maximal value of k_0.

Data S4 Explanation of frequency response analysis results (FRA)

Figure S4 Example of input frequencies for dopamine as used in the simulations (top panels) and the simulated responses (lower panels). The second row shows the dopamine receptor occupancy, the third row the antagonist receptor occupancy and the bottom row the cAMP response for each simulation with the fluctuating dopamine concentrations from the corresponding top row panels. The different line colors represent different simulations for which the dissociation rate constant of the antagonist-receptor complex is changed. The dopamine fluctuation frequencies are indicated above the panels and by the different time scales on the x-axis.

Data S5 Identification of the influence of system-specific parameters on the frequency response analysis results.

Figure S5 Frequency response analysis for 3 different active PDE turnover rate constants and 5 different antagonist k_{off} values. The upper plots show the influence of the antagonist k_{off} for two different active PDE turnover rate constants, and the lower plots show the influence of the active PDE turnover rate constant for two different k_{off} values. The input signal was a sine wave of free dopamine with an amplitude of 10nM and baseline of 20 nM, at the frequencies indicated on the x-axis. At each active PDE turnover rate, 5 different antagonist k_{off} values were simulated, which are represented by the different line colors. The k_{on} values were changed simultaneously with k_{off}, which means that the K_D was constant at 6.93 nM. The antagonist concentration was 14 nM, the LFR_{50} was 1.03 and all system-specific parameters were identical to Table 3.

Figure S6 Frequency response analysis for 5 active PDE-dependent cAMP turnover rate constant (k_3) values and 5 antagonist k_{off} values. The upper plots show the influence of the antagonist k_{off} for two different active PDE turnover rate constants, and the lower plots show the influence of the active PDE-dependen cAMP turnover rate constant for two different k_{off} values. The input signal was a sine wave of free dopamine with an amplitude of 10nM and baseline of 20 nM, at the frequencies indicated on the x-axis. At each cAMP turnover rate, 5 different antagonist k_{off} values were simulated, which are represented by the different line colors. The k_{on} values were changed simultaneously with k_{off}, which means that the K_D was constant at 6.93 nM. The antagonist concentration was 14 nM, the LFR_{50} was 1.03 and all system-specific parameters were identical to Table 3.

Figure S7 Frequency response analysis for 4 different dopamine-receptor k_{off} values and 5 different antagonist k_{off} values. The upper plots show the influence of the antagonist k_{off} for two different active PDE turnover rate constants, and the lower plots show the influence of the dopamine k_{off} for two different antagonist k_{off} values. The input signal was a sine wave of free dopamine with an amplitude of 10nM and baseline of 20 nM, at the frequencies indicated on the x-axis. At each dopamine dissociation rate constant, 5 different antagonist k_{off} values were simulated, which are represented by the different line colors. The k_{on} values were changed simultaneously with k_{off}, which means that the K_D was constant at 6.93 nM. The antagonist concentration was 14 nM, the LFR_{50} was 1.03 the receptor recycling rate constant was switched to 0 and all other system-specific parameters were identical to Table 3.

Figure S8 Frequency response analysis for 4 different antagonist concentrations and 5 different antagonist k_{off} values. The upper plots show the influence of the antagonist k_{off} for two different active PDE turnover rate constants, and the lower plots show the influence of the antagonist concentration for two different antagonist k_{off} values. The input signal was a sine wave of free dopamine with an amplitude of 10nM and baseline of 20 nM, at the frequencies indicated on the xaxis. At each antagonist concentration, 5 different antagonist k_{off} values were simulated, which are represented by the different line colors. The k_{on} values were changed simultaneously with k_{off}, which means that the KD was constant at 6.93 nM. The antagonist concentration was 14 nM, the LFR50 was 1.03 and all system-specific parameters were identical to Table 3.

Figure S9 Sensitivity analysis for 5 different antagonist concentrations (line colours) and for a 10-fold increase and decrease of each parameter from Table 3, the antagonist K_D, k_{off} and the LFR_{50} (panels). The middle panels are the same in the whole figure, representing the parameters in Table 3, an antagonist K_D value of 6.93 nM, an antagonist k_{off} value of 0.1 min^{-1} and an LFR_{50} value of 1.02. The y-axis can change between the different panels.